Bulletin of Glacier Research 12 (1994) 95－104

Monitoring ground surface condition on Tibetan Plateau by using satellite remote sensing

Tosio KOIKE[1], Katsumoto SEKO[2], CHEN Xianzhang[3], Takeo TADONO[1], Katsunori TAMAGAWA[1], Hiroshi IGARASHI[4] and Hideki TAKIZAWA[5]

1 Nagaoka University of Technology, Nagaoka 940－21 Japan
2 Institute of Hydrospheric-Atmospheric Science, Nagoya University, Nagoya 464－01 Japan
3 Lanzhou Institute of Glaciology and Geocryology, Lanzhou, China
4 Institute of Geoscience, University of Tsukuba, Tsukuba 305 Japan
5 Tokyo University of Agriculture and Technology, Fuchu 183 Japan

(Received May 6, 1994 ; Revised manuscript received August 18, 1994)

Abstract

Due to dynamic behavior of the cryospheric parameters on Tibetan Plateau, efficient monitoring is possible only by using satellite remote sensing. The methods for deriving information on snow and ice, clouds, vegetation and soil wetness from satellite data are presented and their applicability is investigated in this paper. Cloud and snow are classified by channel 3 and 4 data of NOAA AVHRR, and the vegetation index is calculated using channel 1 and 2. The Landsat TM image shows the firn line, the accumulation area and the bare ice with the undulating topography on the glacier and the activity of vegetation. Three images of JERS-1 SAR are used for classifying the conditions of ground surface and glacier and detecting their seasonal changes. Snow deposit and melting on the glacier and the temporal and spatial distribution of soil wetness are obtained. The ground surface conditions in the plateau scale are classified by using SSM/I data. The dry snow and very wet areas on January and June are identified by the discrepancy between the SSM/I brightness temperatures at 19GHz and 37GHz.

1. Introduction

The energy and water cycle on Tibetan Plateau has been suggested to play an essential role in the Asian Monsoon system and to affect the global climate. On the other hand, the heat budget and hydrological processes on the plateau are also sensitively controlled by the ground surface conditions. There is large spatial and temporal diversity of ground surface conditions, *i.e.* low vegetated dry or wet surface with permafrost, snow cover, glacier, lake water surface *etc.* However, there are only a few ground observational stations on Tibetan Plateau. Efficient monitoring in the plateau scale is possible only by using satellite remote sensing methods. Therefore it is indispensable to establish the satellite-based observational systems in order to investigate the energy and water cycle on Tibetan Plateau. The areal extent and water equivalent of snow and ice are the essential information for understanding the hydrological cycle on Tibetan Plateau. The climatic distribution of clouds determines the surface radiative heat balance. Vegetation in the periglacial environment is a controlling factor of hydrological cycle. The distribution of vegetation is an index of on-going climatic change and it is possibly related with the activity of permafrost. Ground-based and satellite-based observaions were conducted on Tibetan Plateau for developing algorithms for the cryospheric parameters and evaluating their applicability.

2. Measurement of spectrum albedo

Spectrum albedo of ground surfaces including glacier were measured in the intensively studied period occasionally. We have tried to get simultane-

ous ground truth corresponding to satellite optical sensors. Although all trials were in vain due to clouds, seasonal change of spectral reflectance of ground surface was obtained and it will be used as basic data for future remote sensing studies in this region. Instrument used in this study is 'Personal spectrometer II' manufactured by Analytical Spectral Devices Inc., which can measure spectral albedo from 380 μm to 1080 μm with 1.38 μm interval. White reference board was used for the measurement. Albedo spectra of snow and ice on the glacier and vegetated ground in permafrost area were measured several times in the intensive study period. Albedo spectra on the glacier were measured and shown in Seko *et al.* (1994). The spectra are affected by several metamorphosing process from new snow to granular snow and impurities. Reduction of albedo in near-infrared region is caused by the variation of grain size and one in shorter wave length less than 600 μm shows the effect of impurities mainly composed by mineral dust. Spectral albedo on vegetated grounds was measured several times in Tanggula mountains as shown in Fig.1, where continuous meteorological observation has been carried out from June to September, 1993 (Ohata *et al.*, 1994). Figures 2a and 2b show the albedo spectra of the ground surface at Wetland and D105 respectively. The surface is covered by short grass. The density of vegetation is higher in Wetland than in D105. There is a distinct change of spectrum. On 16 June, ground surface was covered by yellow grass which is in premature stage of plant growth. On 25 July, the color of the grass turned into brilliant green. Corresponding to the changed color of leaves, we can notice an apparent absorption near 670 μm (by Chlorophyll) and great contrast between the strong absorption and high reflectivity in near infrared region.

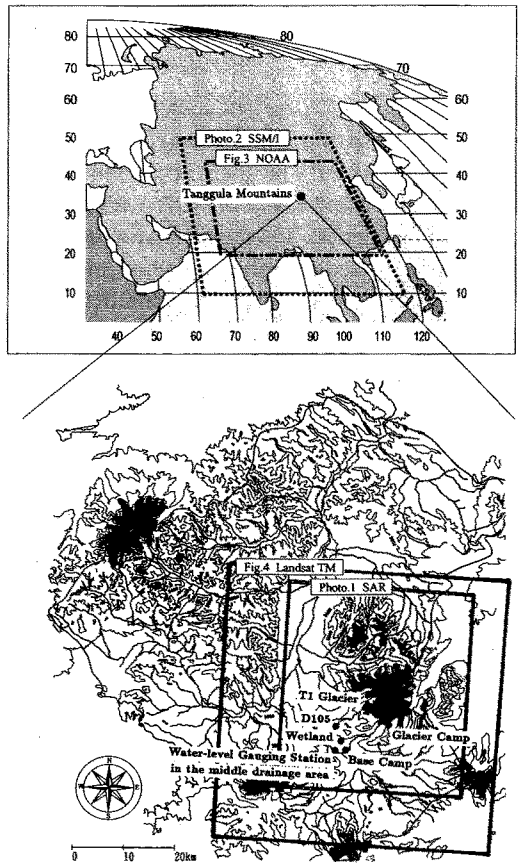

Fig. 1. Study area and coverages of satellite data.

3. Examples of satellite images

3.1 NOAA AVHRR

We should discriminate high reflectance object such as clouds or snow and ice from other surfaces by using single channel albedo on Ch1 (channel-1 ; 0.6−0.7 μm). Then, cryosphere and cloud can be distinguished by using mid-infrared channel (channel-3 ; 3.6−3.9 μm). Low albedo surfaces are analyzed by using Normalized Differential Vegetation Index (NDVI) and thermal infrared brightness temperature (Tb) on Ch4 (channel-4 ; 10.5−11.5 μm). Classification of cloud and snow is difficult only by using single channel albedo or brightness temperature. In mid-infrared channel, reflection from clouds is generally higher than that from snow and ice because its smaller grain size of ice particles consisting clouds. By taking the difference of Tb on Ch3 from Tb on Ch4, we can distinguish clouds from snow even if they have wide ranges of temperature. NDVI is calculated by using Ch1 and Ch2 (near infrared, 0.7−1.1 μm) as follows ;

$$NDVI = \frac{Ch2 - Ch1}{Ch2 + Ch1} \quad (1)$$

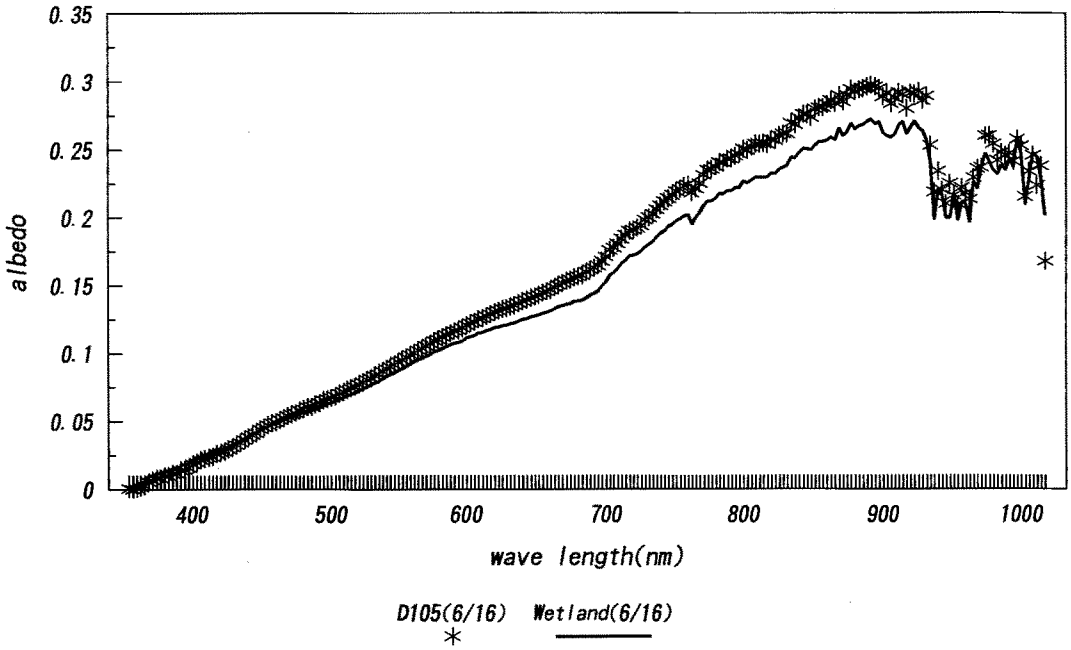

a)June, 16, 1993

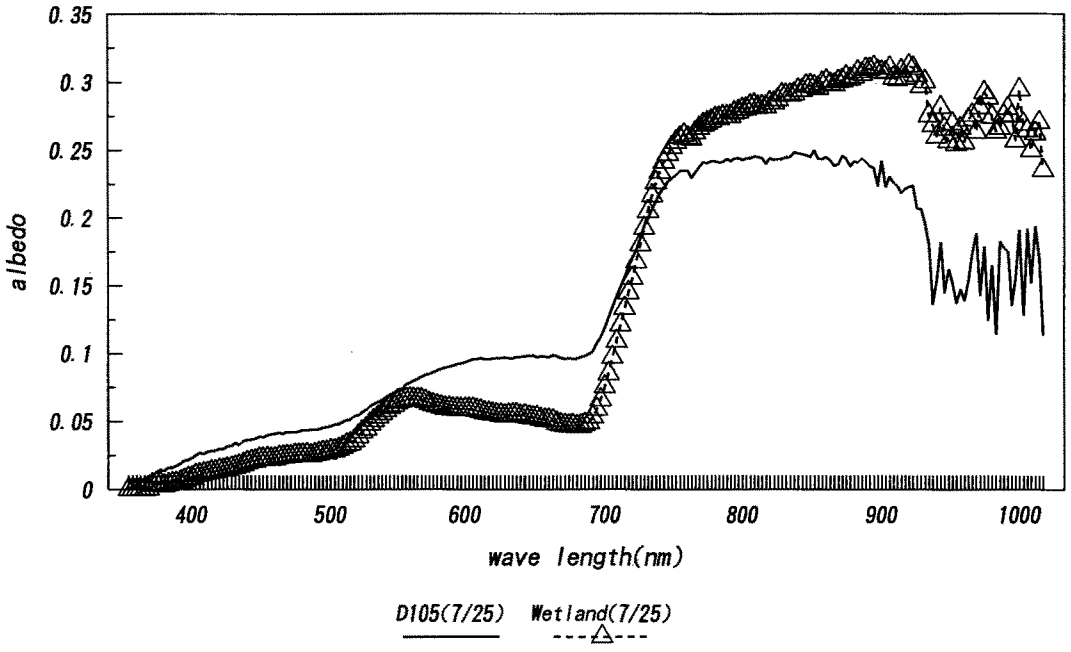

b)July, 25, 1993

Fig. 2. Albedo spectra measured at D105(rather arid surface) and Wetland (very wet surface) measured on ;

Figures 3a and 3b show images in 1.1 km mesh AVHRR data retrieving albedo in Ch1 and NDVI. The coverage of study area is shown in Fig. 1. In the visible image of Fig. 3a, distribution of cryosphere is clearly seen. Vegetation index on the plateau of Fig. 3b represent wide variety of surface condition due to the annual precipitation amount ranging 2 orders of magnitude from several thousands millimeter in the south-western part of the plateau to a few tens of mm in north-western part.

3.2 Landsat TM

Figures 4a and 4b show the images of Landsat TM in single channel albedo (channel-2 ; 0.52－0.6 μm) and normalized vegetation index encompassing Middle drainage area as shown in Fig. 1(Ohta *et al.*, 1994), respectively. The coverage of LANDSAT TM image is expressed in Fig. 1. Firn line is clearly revealed by the apparent difference in albedo. CCT count, which corresponds to refrectivity, in the four channels from visible to near-infrared and spectral ratio of each channel to Ch1 along a flow line of T1 Glacier are shown in Fig. 5a and Fig. 5b, respectively. Spectral ratio between visible and near-infrared region is a good indicator of surface conditions such as snow or ice. An apparent change in the spectral ratio is seen at 3600 m and it clearly shows firn line in the winter, 1990, while fluctuations in the reflectivity exist in each channel in the accumulation area associated with the undulating topography on the gla-

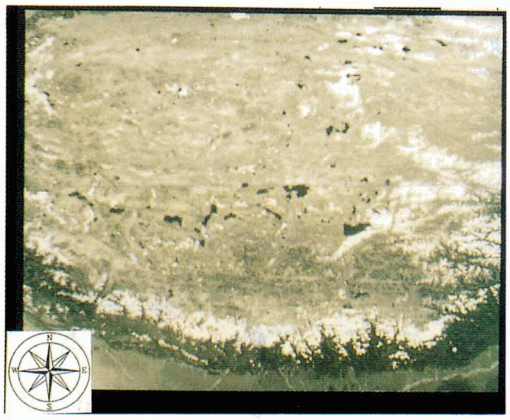

a) albedo in channel-1

b) normalized differntial vegetation index(NDVI) using channel-1 and -2 of NOAA AVHRR.

Fig. 3. NOAA AVHRR images taken on Nov. 20, 1990.

a) albedo in channel-1

b) normalized vegetation index in Landsat TM ; the definition of NDVI in Landsat TM is described in the text.

Fig. 4. Landsat TM images taken on Jan. 20, 1990.

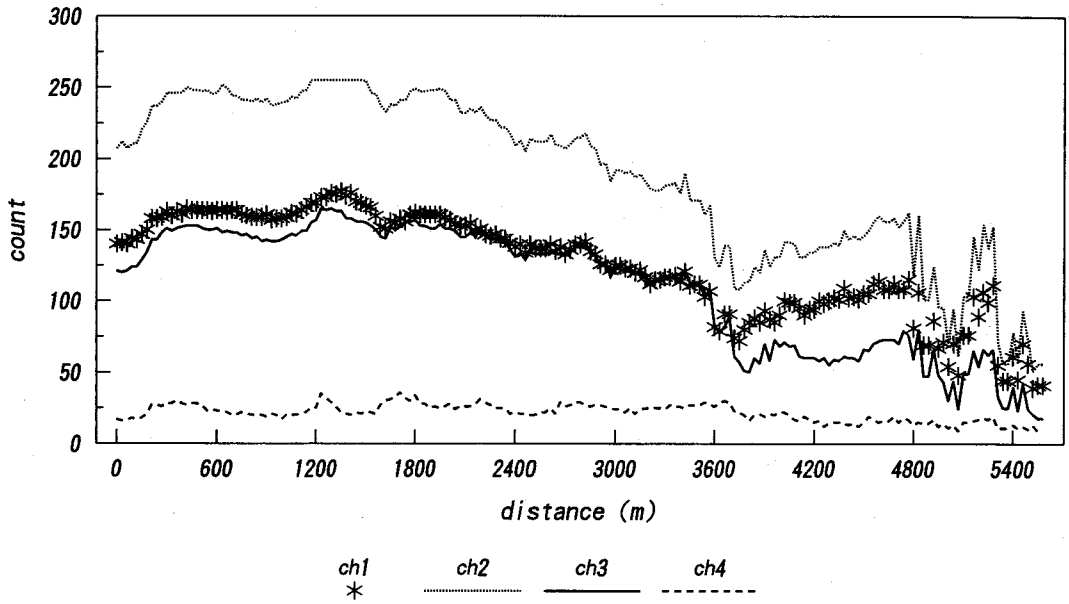

a) CCT count in each channel from ch-1 to ch-4

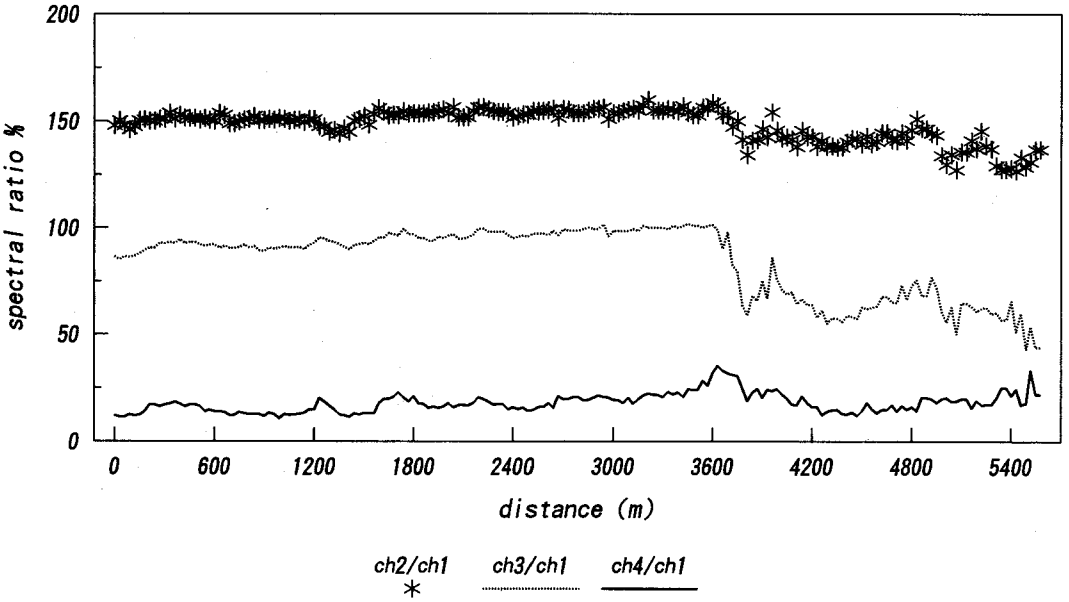

b) spectral ratio between each channel

Fig. 5. Profile of CCT count of reflectance from a glacier surface (T1 glacier) in Landsat TM. X-axis means the distance from the top of the glacier.

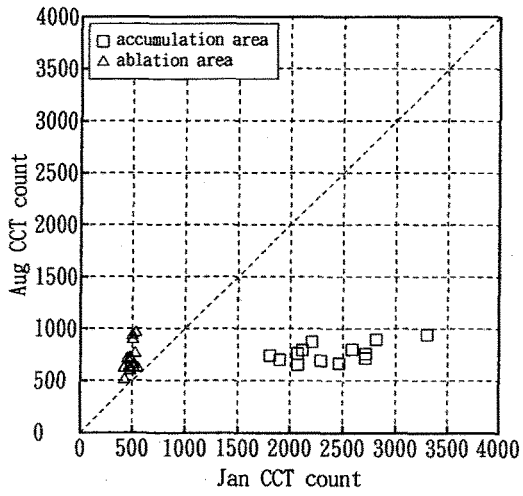

a) On a glacier.

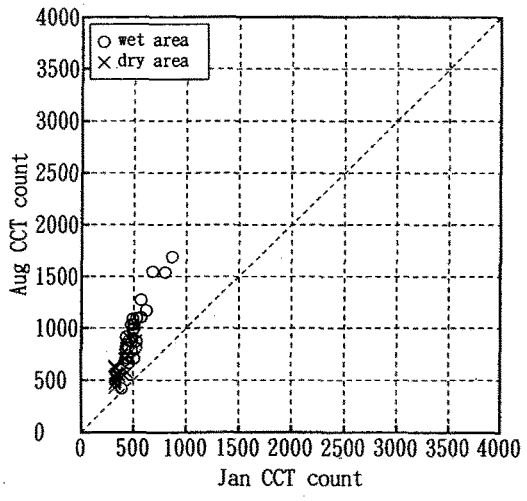

b) On snow-free region.

Fig. 6. CCT counts on the various surface on January and August in JERS-1 SAR.

ciers. It is interesting from a climatological point of view that bare ice is exposed even in winter season. Albedo in each channel on the ablation area further than 3600 m is about half of that on the accumulation area. Figure 4b shows the distribution of vegetation index including middle drainage area. Vegetation index in Landsat TM data were calculated by using count number in visible wave length (channel-2 ; 0.52−0.6 μm) and near-infrared wave length (channel-4 ; 0.76−0.9 μm) as follows ;

$$VI=\frac{Ch4-Ch2}{Ch4+Ch2} \quad (2)$$

While activity of vegetation was low in winter when this image was taken, there is remarkable variation of vegetation index in this area. It is located in the valley at the east side of glaciers where the value of vegetation index is very high. In Dongkemadhi valley, there are several areas where *VI* value is very high. The distribution of vegetation is possibly controlled by precipitation and/or permafrost. Total summer precipitation amount at Glacier Camp(5500 m) is estimated to be nearly 1.4 times of that at Base Camp(5060 m)(Ueno *et al.*, 1994). Difference of precipitation between each valley does not seem to be so great to cause such variety of surface condition. It is considered that the distribution of vegetated area is controlled by soil moisture content and it is probably related with the behavior of active layer of permafrost (Yabuki *et al.*, 1994).

3.3 JERS-1 SAR

Photo 1, which corresponds to the area as shown in Fig. 1, shows the processed JERS-1 SAR image in Tanggula mountains. The speckle noise of the original images are eliminated by using the low pass filter. Both images on January and May are overlaid on the August one using 3-dimensional Affine transformation and the nearest neighbor interpolation. Surface conditions are identified based on the Landsat TM image and the field observation. The blue area corresponds to the accumulation area of the glacier. The yellow and red area is very wet in summer and very rough with earth hammock. Figures 6a and 6b show CCT counts on January and August, 1993 on a glacier and snow-free region. CCT count of SAR corresponds to the magnitude of the back scattering coefficient. On the upper part of the glacier the CCT counts in winter are much larger than in summer. It is considered to be the effect of volume scattering of winter dry snow on the glacier. CCT counts of the wet and rough surface are larger than ones of the dry and flat surface on both months. The ground surface is perfectly frozen and dry in winter. The discrepancy between the CCT counts on two surfaces in winter would be caused from the surface roughness of earth hammock. In summer the surface of permafrost becomes melting and soil moisture increases in both area. That is why August CCT counts in both area is higher than January CCT counts. However, the surface coverd with earth hammock is much

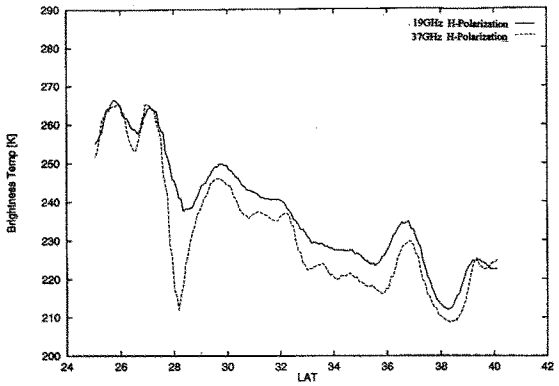

a) January, 1989.

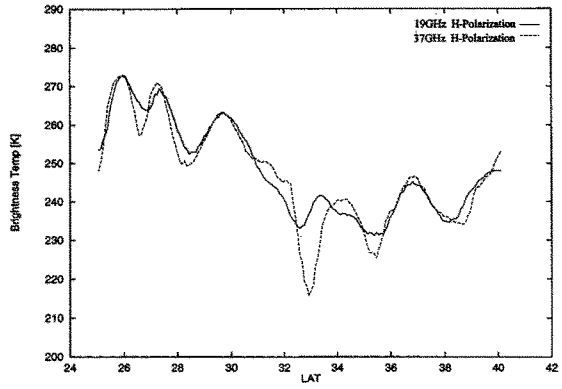

b) June, 1989.

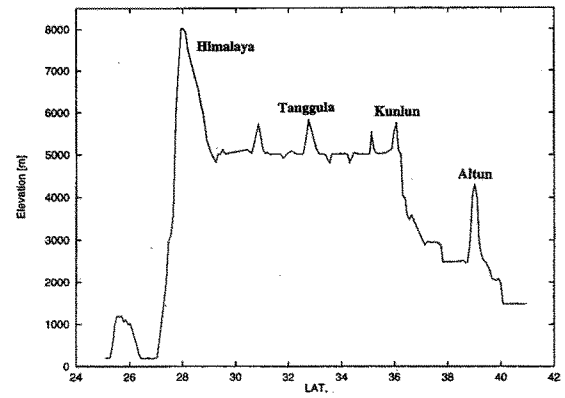

c) Altitudinal distribution.

Fig. 7. Spatial and seasonal distribution of the brightness temperature at 19GHz and 37GHz along the longitude 91 degree east.

wetter in summer than the other. The discrepancy of CCT counts of two surface conditions in summer expresses the coupled effect of soil moisture and surface roughness.

It is interesting to note that back scattering coefficient of SAR image in summer shows similar distribution to that of the vegetation index. A future problem is to investigate the relationship between vegetation on the ground surface and sub-surface condition including soil moisture affected by permafrost by using multi-sensors in different wave length.

3.4 DMSP SSM/I

The annual SSM/I data set was developed by using every 5 days raw data in 1989. The original data was geometrically corrected and resampled to 10 by 10 km pixels. The values of the brightness temperature were averaged at the overlaid pixels with more than two orbital data.

Figures 7a and 7b show the spatial and seasonal distribution of the brightness temperature at 19GHz and 37GHz along the longitude 91 degree east from lower latitude to higher latitude on January and June, respectively. Elevation distribution along the line is shown in Fig. 7c. There is the largest discrepancy between the brightness temperatures at two frequencies around Himalaya region at about 28 degree north on January. We can find smaller discrepancy over the Tibetan Plateau. Figure 8 shows the microwave emissivity of snow at each frequency(Rott, 1987). The emissivity of dry snow is similar to one of the snow-free surface at the low frequency. On the other

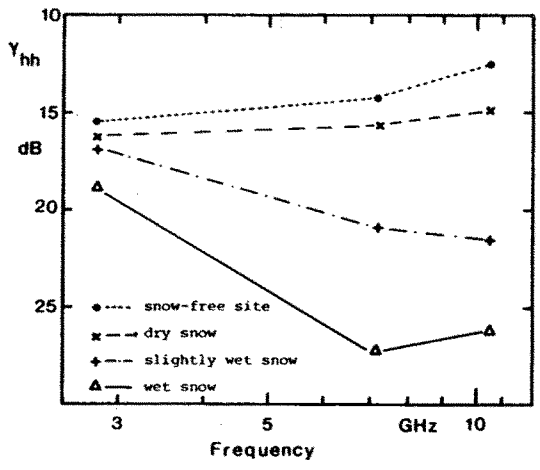

Fig. 8. Microwave emissivity of snow(Rott, 1987).

Photo 1 JERS-1 SAR images in Tanggla mountains.

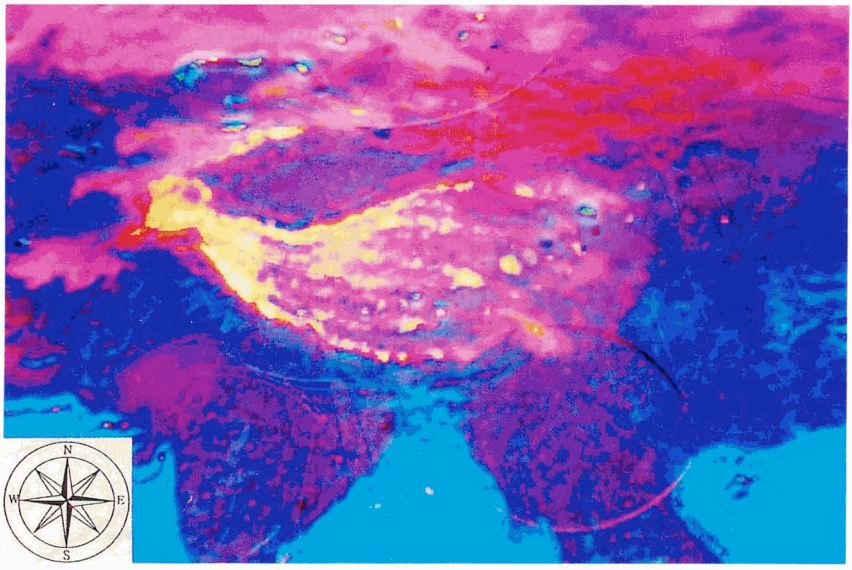

Photo 2 Classification of the ground surface conditions by using the SSM/I data on January and June, 1989. (yellow : dry snow covered region both on January and on June, pink : snow covered region on January and snow-free on June, blue : wet region on June).

hand the former becomes lower than the latter at higher frequency because of the volume scattering. Therefore, the discrepancies as shown in Fig.7a mean that the area is covered with dry snow. Futhermore, the magnitude of discrepancy corresponds to the water equivalent of dry snow. Also we need to take into account of the effect of snow particle size on volume scattering. On June the discrepancy around Himalaya mountains disappears as shown in Fig. 7b. We can find the signal of dry snow in the central and northern part of Tibetan Plateau. On the southern part of Tibetan Plateau from 31 to 32 degree north, the relationship becomes opposite, *i.e.* the brightness temperature at 37GHz is larger than one at 19GHz. It shows that the surface condition of this area becomes very wet by melting snow or permafrost with strong solar radiation or by the effect of monsoon precipitation, scince the lower frequency is more sensitive to surface soil moisture. Photo 2 shows the result of classification of the ground surface conditions by using the data on January and June in the region as shown in Fig. 1. The yellow area corresponds to the dry snow covered region both on January and June. Pink color shows the area which is covered with dry snow on January and snow-free on June. Blue area is wet region on June. We can find some wet regions on Tibetan Plateau.

4. Use of remote sensing on Tibetan Plateau

The cryospheric parameters on Tibetan Plateau are needed to be monitored by satellite remote sensing. The classification of snow and ice, clouds and the various types of snow-free ground surfaces was made by multi-spectral analyses of the optical sensors such as NOAA AVHRR and LANDSAT TM. Furthermore, the surface conditions of the ground and glacier were observed by the microwave sensors such as JERS−1 SAR and DMSP SSM/I. Microwave techniques offer important advantages for mapping the ground surface in the cryosphere. One is the all weather capability and the other is the possibility to detect soil wetness and snow water equivalent.

NOAA AVHRR data can provide images of the whole part of Tibetan Plateau. 1.1 km of resolution of AVHRR is enough to discriminate valley-ridge topography on the plateau. We can detect clouds, snow covered area including glaciers and vegetation by using multi-spectral information of AVHRR.

High spatial resolution images such as Landsat TM, and MOS1 MESSR are useful for mapping heterogeneous ground surface in the intensively studied drainage area of Cryosphere Research on Qingzang Plateau(CREQ). The spectral information of these sensors can be utilized for many purposes as follows. On a glacier, its area, firn line and albedo can be detected. Using thermal infrared channel of Landsat TM, we can derive surface temperature of glaciers and ground. In periglacial area, near infrared reflectance is available for mapping vegetation, permafrost and surface soil moisture. Interpretation of SAR images needs the information from the visible and near infrared channels. Usage of the high spatial resolution optical sensors is generally limited due to cloud, especially in monsoon season.

The synthetic aperture radars which are mounted on satellites such as the ERS-1 and the JERS-1 are expected to observe the surface hydrological conditions in detail. This study focuses on the soil moisture, snow and snow-free and surface roughness. The back scattering coefficient measured by microwave sensors is affected not only by soil moisture and snow but also the other factors such as polarization, incident angle, sensor's frequency, surface roughness, soil composition *etc.*. For classifying the surface condition and detecting its seasonal change, it is considered to be effective to overlay several SAR images together.

SSM/I has the wide observational swath and the short recurrence period and overcomes the problems of polarization mixing and antenna side-lobe. We can identify the dry snow area and the very wet area using the discrepancy between the SSM/I brightness temperatures at 19GHz and 37GHz based on the characteristics of volume scattering and surface scatering, respectively.

References

1. Ohata, T., Ueno, K., Endho, N. and Zhang Y. (1994) : Meteorological observation in the Tanggula Mountains, Qingzang (Tibet) Plateau from 1989 to 1993, Bull. Glacier Res., **12**, 69−75.
2. Ohta, T., Yabuki, H., Koike, T., Ohata, T. and Zhang Y. (1994) :Hydrological observations in the Tanggula Mountains, the Tibetan Plateau-discharge, soil moisture and ground temperature-. Bull. Glacier Res., **12**, 49−56.
3. Rott, H. (1987) :Remote Sensing of Snow. IAHS Publ., **166**, 279−290.
4. Seko, K., Pu J., Fujita, K., Ageta, Y., Ohata, T. and Yao T. (1994) : Glaciological observations in the Tanggula Mts., Tibetan Plateau. Bull. Glacier Res., **12**, 57−67.

5. Ueno, K., Endo, N., Ohata, T., Yabuki, H., Koike, T., Koike, M., Ohta, T. and Zhang Y. (1994) : Characterisitics of precipitation distribution in Tanggula, Monsoon, 1993. Bull. Glacier Res., **12**, 39−47.
6. Yabuki, H, Ohata, T., Ohta, T., and Zhang Y. (1994) : Measurements of ground temperature and soil moisture content in the permafrost. area in Tanggula Mountains, Tibetan Plateau Bull. Glacier Res., **12**, 31−38.